Revista Mexicana de Astronomía y Astrofísica, **38**, 279–288 (2002)

DENSITY GRADIENTS AND INTERNAL DUST IN THE ORION NEBULA

L. Binette,[1] D. I. González-Gómez,[1] and Y. D. Mayya[2]

Received 2002 June 10; accepted 2002 September 13

RESUMEN

La estructura de ionización de la nebulosa de Orión puede ser descrita como una piel delgada sobre la superficie de una nube densa. Proponemos que una estratificación en la densidad, descrita por una ley de potencias ($n \propto x^{-2}$, donde x es la distancia al frente de ionización), presenta propiedades que concuerdan con nuestros espectros de rendija larga de la nebulosa de Orión. Por ejemplo, existe una relación de unicidad entre el brillo superficial en Hβ, o la densidad del frente de ionización en [S II], y la escala L de la ley de potencias, donde L es la distancia entre el frente de ionización y el lugar donde comienza a crecer la densidad, cerca de la estrella excitadora. Es necesario incluir polvo interno a fin de obtener un ajuste aceptable a las observaciones tanto de la densidad del [S II], como del brillo superficial en Hβ. Los modelos que incluyen granos de polvo pequeños proporcionan un mejor ajuste que aquellos con granos grandes. Los gradientes de los cocientes de líneas observados a lo largo de la rendija se reproducen cualitativamente por nuestros modelos de densidad estratificada, suponiendo una temperatura estelar de 38,000 K. La desexcitación colisional parece ser la responsable de la mitad del gradiente observado en el cociente [N II] $\lambda\,5755$/[N II] $\lambda\,6583$, el cual es sensible a la temperatura. Proponemos que la relación empírica encontrada por Wen & O'Dell (1995) entre la densidad y la distancia a la estrella puede deberse a una estratificación de la densidad en forma de ley de potencias.

ABSTRACT

The ionization structure of the Orion nebula can be described as a thin ionized skin on the surface of a dense cloud. We propose that a steep density stratification, described by a power law ($n \propto x^{-2}$, where x is the distance from the ionization front), exhibits properties which agree with our long-slit spectrum of the Orion nebula. For instance, there exists a unicity relation between both the Hβ surface brightness or the ionization front [S II] density, and the scale L of the power law, where L is the distance between the ionization front and the onset of the density near the exciting star. Internal dust is required to obtain a simultaneously acceptable fit to both the [S II] density and the Hβ surface brightness observations. Nebular models containing small dust grains provide a better fit than large grains. The line ratio gradients observed along the slit are qualitatively reproduced by our density stratified models, assuming a stellar temperature of 38,000 K. Collisional deexcitation appears to be responsible for half of the gradient observed in the [N II] $\lambda\,5755$/[N II] $\lambda\,6583$ temperature sensitive ratio. We propose that the empirical relationship found by Wen & O'Dell (1995) between density and stellar distance may possibly be due to a power-law density stratification.

Key Words: **ISM: DUST — ISM: INDIVIDUAL: ORION NEBULA — ISM: H II REGIONS — LINE: FORMATION**

[1]Instituto de Astronomía, Universidad Nacional Autónoma de México, México.

[2]INAOE, Tonantzintla, México.

1. INTRODUCTION

It was recognized early on by Münch (1958) and Wurm (1961) that the Orion nebula is better described as a photoionized skin on the surface of a dense cloud than by a uniformly filled gas structure. Furthermore, kinematics of the ionized gas (see review by O'Dell 1994) indicates that the gas is flowing away from the dense ionizing front on the surface of the molecular cloud. Although earlier studies proposed an exponential function to describe the density behaviour from such a flow (Tenorio-Tagle 1979; Yorke 1986), more recent theoretical and observational works (Franco, Tenorio-Tagle, & Bodenheimer 1989, 1990; Franco et al. 2000a,b) indicate that expanding H II regions are well described by a power law density stratification $n \propto x^{-\beta}$ with exponents larger than $\beta = 1.5$. This is qualitatively consistent with the results obtained from hydrodynamic calculations of photoevaporative flows from proplyd disks by Richling & Yorke (2000) or from spherical surfaces by Bertoldi (1989) and Bertoldi & Draine (1996). The present paper looks at how the observed gradient of the [S II] density in Orion can be accounted for using a simple power-law density model, and how well the surface brightness compares with the long-slit observations presented here. The aim is to explore the benefits of a power-law density stratification in the context of a determination of the shape of the ionization front (hereafter IF) using a surface brightness map in Hα, a task first performed by Wen & O'Dell (1995) for the two cases of isochoric and exponential density behaviour.

2. OBSERVATIONS AND DATA REDUCTION

We have taken long-slit spectra of the central region of Orion at the Observatorio Astrofísico Guillermo Haro, Cananea, on the 1998 December 21 using a 1024×1024 TEK CCD detector mounted on a Boller & Chivens spectrograph. We used a grating of 300 l/mm and covered the wavelength range 3600–5200 Å, 5500–7100 Å, and 8000–9600 Å in three settings. The corresponding exposure times were 90, 60 and 300 seconds, respectively. A slit width of $2\farcs5$ was used. The effective spectral resolution was ≈ 6 Å. The slit was aligned West-East and off-centered by $30''$ to the South of θ^1 C Ori as illustrated in Figure 1. Arc spectra were taken as well as standard star exposures. Data reduction (bias subtraction, flat fielding, wavelength and flux calibration) was performed with IRAF.[3] Due to non-photometric

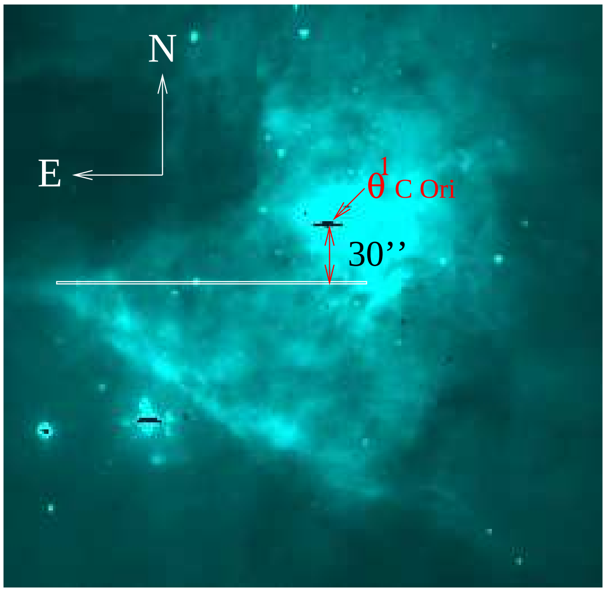

Fig. 1. Image illustrating the position of our long-slit on an R-band image of Orion. The position of the exciting star θ^1 C Ori (whose image is saturated) is indicated. The R-band filter encompasses Hα and the red [N II] lines which account for most of the nebular emission visible on the image.

conditions and partial cloud coverage, we could not derive a reliable absolute flux calibration. We hence used the calibration of Rodríguez (1999), who had also observed with the slit aligned East-West with her regions A-1 and A-3 common to ours. We tied our Hβ fluxes to the mean surface brightness within her region A-1. In any event, the adopted Rodríguez surface brightness value is only 25% higher than our initial calibration. Line fluxes were reddening corrected using the Balmer decrement and the Galactic reddening law (Seaton 1979). Further details on the data can be found in González-Gómez (1999).

3. THE PHOTOIONIZATION MODELS

We adopt a similar approach to that of Binette & Raga (1990, hereafter BR90) who studied the properties of power-law densities in photoionized slabs (see also Williams 1992). However, we adapted their simple slab geometry to the more appropriate spherical geometry for reasons given below in § 3.2. Another paper which considers power-law density stratification in photoionization models is that of Sankrit & Hester (2000) (see also Hester et al. 1996).

The emission line measures in Orion are dominated by the gas near the IF as a result of the strong

[3] IRAF is the Image Reduction and Analysis Facility made available to the astronomical community by NOAO, which are operated by AURA, Inc., under contract with the US National Science Foundation.

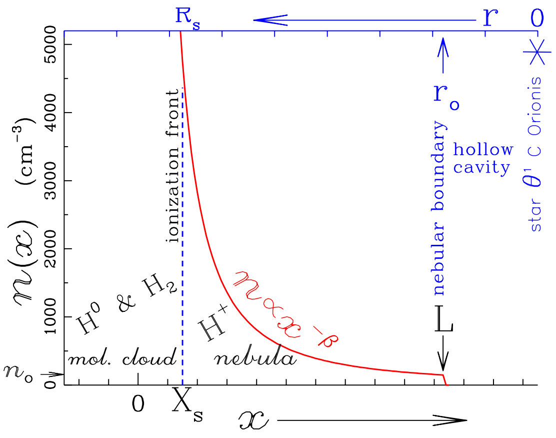

Fig. 2. Diagram qualitatively illustrating our power-law density stratification as a function of x. The origin of the spatial x-axis lies at a depth L from the nebular boundary and the density at that position (at $x = L$) is labelled n_0 (see equation (1)). Note that L will be allowed to vary with angular direction from θ^1 C Ori. The top axis is the radial distance r from the star θ^1 C Ori, with r increasing towards the left. The IF (or inner Strömgren boundary) is situated at X_s (or equivalently at R_s). The electronic density inferred from the [S II] doublet corresponds to a density near the IF. The hollow gas cavity surrounding the star has a size r_0. In our models, the adopted value for r_0 is much smaller than depicted above.

density gradient towards it. In the work of Wen & O'Dell (1995, hereafter WO95), the authors approximated the front structure as gas segments (or columns) aligned towards *our* line of sight with a projected area on the sky of $2'' \times 2''$. In their final best model, the densities within the segments declined exponentially towards the observer rather than radially towards θ^1 C Ori. Using the observed distribution of Hα surface brightness and [S II] gas density, WO95 were able to solve for the IF distance (along our line of sight) for the whole nebula. Such a distribution of distances is termed the "shape" of the IF. The gas segments of their model did not extend up to the exciting star, a characteristic also shared by the isobaric slab model of Baldwin et al. (1991, hereafter BF91). In such a scheme, the segments are independent and a density must be specified for each segment. In this paper, we will explore density distributions that are exclusively a function of radius from θ^1 C Ori, without assuming any significant gas cavity near θ^1 C Ori.

3.1. *The Radial Density Gradient*

We adopt a similar notation to BR90 in which the density profile (with an origin lying inside the dense cloud) is described as follows:

$$
\begin{aligned}
n(x) &= n_0\,(L/x)^{\beta} \quad &\text{for } x \le L,\\
n(x) &= 0 \quad &\text{for } x > L,
\end{aligned}
\qquad (1)
$$

where $n(x)$ is the gas density, β the power-law index ($n \propto x^{-\beta}$), n_0 the boundary density of the nebula towards the exciting star, and x the variable representing the distance from the inner density discontinuity at $x = 0$. Note the reversal of axes relative to traditional studies: the ionizing radiation is entering at the cloud boundary $x = L$ and is absorbed inward up to the inner Strömgren boundary at X_s (see Figure 2). The steep density gradient near the origin ensures that the photons are absorbed before the density discontinuity, hence $X_s \gtrsim 0$.

In the case of Orion, the spherical geometry is necessary in order to take account of the geometrical dilution of the ionizing radiation across the radial density structure. One can define the variable r as the distance from the central ionizing star; that is $r = L - x + r_0$ where r_0 is the radius of the central hollow cavity and n_0 the gas density at r_0. When the ionizing photon luminosity $Q_{\rm H}$ is sufficiently high (or the density n_0 low), the Strömgren radius, $R_s = L - X_s + r_0$, is near the origin of the x-axis, at a distance $\simeq L + r_0$ from the exciting star (since X_s is negligible). This is referred to by BR90 as the "strong gradient" regime. In the converse case, for very low ionizing photon luminosities $Q_{\rm H}$ (or for high boundary densities n_0), R_s shrinks (X_s becomes non-negligible) and becomes of order r_0 plus small fraction of L, a condition which BR90 labeled "weak gradient" because the nebula's thickness is smaller than the scale of the density gradient L. All the quantities introduced above are illustrated in Fig. 2.

The "strong gradient" regime is the appropriate one for Orion since the nebula is traditionally approximated by a skin-like structure on the face of a dense molecular cloud (BR90; O'Dell 1994). One advantage of the power-law stratification when the regime of "strong gradient" prevails is that we know beforehand the approximate radius of the IF ($\lesssim L + r_0$). In the case of an exponential stratification, which is much shallower than a power law, it requires solving for the ionizing radiation transfer inside the nebula in order to predict the IF depth.

To be specific, we will consider the case of a power-law index $\beta = 2$. Very similar nebular line ratios of [O II], [O III], etc., were obtained with indices of $\beta = 1.5$ and 1.0, provided we adjusted n_0 and L in such a way that both the ionized depth R_s and the [S II] density remained the same as that obtained with the $\beta = 2$ case. We consider that our results do not depend on the particular choice of β made here.

We found no justification for having an arbitrary large region devoid of gas around θ^1 C Ori and so have set $r_0 = 0.007$ pc $\lesssim 0.05R_\mathrm{s}$, a size so small that its precise value has no impact on the calculations.

3.2. *The Geometry*

The geometry of the IF is highly structured and complex (cf. WO95) and cannot be modeled directly by a code like MAPPINGS IC which is designed to handle simple nebular geometries. Our approach has been to compute a sequence of spherical models of different scale L, cf. equation (1), in order to simulate small areas of the IF located at different distances from the exciting star. This piecewise approach (a different model for each position along the slit) allowed us to reconstruct the IF contribution through each aperture element. To account for the projection of each slit aperture element onto the calculated Strömgren spheres, we used MAPPINGS IC to carry out the integral of line emissivities over spatial limits corresponding to the appropriate aperture projection onto the calculated spheres.

Our aim is to model only the background IF (the component B in BF91), which is much brighter than the foreground IF (the component A in BF91). We therefore halved the fluxes computed by MAPPINGS IC to reduce the geometry to that of a hemisphere rather than a sphere. Furthermore, to remove the small contribution due to component A, we multiplied the *observed* Hβ surface brightness by 4/5, the same value as in BF91.

To sum up, the different IF positions covered by the slit are associated with a sequence of models that differ only by their value of the scale L. Since our slit was offset to the South by $30''$ from θ^1 C Ori (extending mostly eastward), it did not sample gas components which overlapped along common radial lines from the exciting star.

3.3. *Metallicity, Dust, and Q_H*

Dust mixed with nebular gas, a possibility studied by BF91, could play an important role in the structure of the Orion nebula. We define μ_D as the amount of dust (by mass) present in the gas in units of the solar neighborhood value. The code MAPPINGS IC includes the effects of internal dust as described in Binette et al. (1993). We will consider two extinction curves, which present quite different behaviors in the far-UV, both calculated by Martin & Rouleau (1991): (a) the *orion* curve[4] used by BF91 is characterized by a population of relatively large grain sizes covering the range 0.03–0.25 μm, (b) the *noiro* curve, first introduced by Magris, Binette, & Martin (1993), is characterized by a population of small grain sizes covering the range 0.005–0.03 μm. A possible justification is that photoerosion, which is significant in photoionized gas, could have the effect of reducing the mean grain size to that characterizing the *noiro* curve. Interestingly, a distribution of small grains may also play an important role in resolving the temperature problem in H II regions (Stasińska & Szczerba 2001). Note that the solar neighborhood extinction curve as calculated by Martin & Rouleau (1991) is composed of grain sizes covering the full range 0.005–0.25 μm (i.e., *ism* = *orion* + *noiro*). The advantage of using the *noiro* and the *orion* curves is that they provide a simple characterization of fairly opposite cases regarding extinction properties in the UV.

We adopt the same gas phase abundances as those determined by BF91 (mean metallicity at $0.7 Z_\odot$) and the stellar atmosphere models of Hummer & Mihalas (1970) with $T_\mathrm{eff} = 38,000$ K, using the scheme proposed by Shields & Searle (1978) to interpolate in effective temperature and metallicity between atmosphere models. The choice of temperature is discussed in § 4.3.

As argued by WO95, the observed recombination line surface brightness includes a reflected back-component due to scattering from the background dusty molecular cloud. To correct for this, as in WO95, we multiplied the observed Hβ surface brightnesses by 2/3 and adopted a reduced stellar photon luminosity of $Q_\mathrm{H} = 10^{49}$ photons s-1 in the models (see discussion in WO95).

4. RESULTS OF THE MODELS

Our main proposition is that only one basic variable of the nebular geometry, the scale L, varies behind the slit aperture. We will show that the observations we have taken, albeit very limited, are *not* inconsistent with this simple picture.

4.1. *Properties of a Power-Law Stratification*

For a given dust content μ_D and dust extinction curve, we proceed to show that for a given value of

[4] The *orion* extinction curve is certainly indicated for the cold gas in front of the Orion nebula (inside the "Lid") but is not necessarily appropriate for the warm ionized gas.

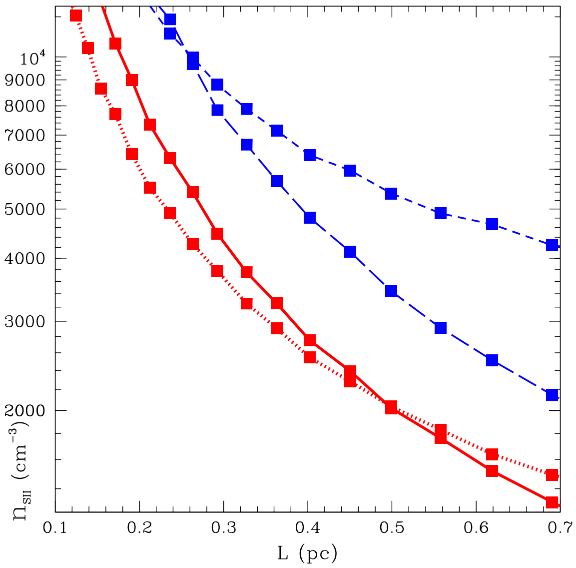

Fig. 3. Behavior of the density inferred from the [S II] lines as a function of the scale L employed in different photoionization calculations (each model is represented by a filled square). The long-dashed and short-dashed line represent two dust-free sequences of models in which the boundary density is $n_0 = 150$ and $2000\,\mathrm{cm}^{-3}$, respectively. The dotted and solid lines represent dusty models (all with a boundary density $n_0 = 150\,\mathrm{cm}^{-3}$) in which the *orion* ($\mu_\mathrm{D} = 0.8$) or the *noiro* ($\mu_\mathrm{D} = 0.4$) extinction curve was employed, respectively.

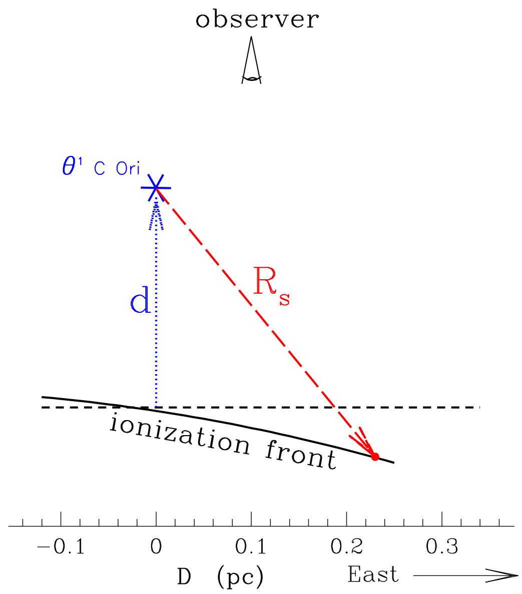

Fig. 4. Figure illustrating the sky projection of the West-East aligned slit onto the nebular IF. The distance between θ^1 C Ori and the IF is R_s. The substellar distance is d (see § 4.2). There is a further offset of the slit to the South of θ^1 C Ori of 0.073 pc (not shown).

n_0, there exists a unicity relation between the [S II] density (which is representative of the IF electronic density) and the scale of the gradient L. This is shown in Figure 3, where we plot the [S II] density as a function of the power-law scale L employed in different photoionization calculations.

In the dust-free case, the long-dashed line corresponds to the sequence of models with $n_0 = 150\,\mathrm{cm}^{-3}$, while the short-dashed line corresponds to models with a higher boundary density $n_0 = 2000\,\mathrm{cm}^{-3}$. For the denser model, the density gradient is much too shallow, since we get a R_s of only 0.25 pc in the model with $L = 0.7$ pc. Clearly, the parameter n_0 plays an important role. Its value can be deduced by requiring that the best model sequence fits simultaneously the observed profiles along the slit in Hβ brightness and in [S II] density.

In Fig. 3, the dotted line represents the case of using the *orion* extinction curve with $\mu_\mathrm{D} = 0.8$ (this sequence of models have the same dust characteristics as those assumed by BF91). The use of the smaller grains *noiro* curve (solid line) on the other hand causes a considerable change in the inferred position of the IF even though these models contain only *half* the mass of grains present in the *orion* curve models (dotted line). The reduction of the IF radius is due to the amount of ionizing photons absorbed by the dust grains.

In their determination of the IF shape, WO95 found a very interesting, albeit unexplained, relationship between the distance to θ^1 C Ori and the gas density (their Fig. 6). They also found that the closer the IF is to θ^1 C Ori, the higher the Hα brightness appears to be. As shown in Fig. 3, a power-law stratification establishes a relationship between the scale L and the [S II] density near the IF. A similar relationship holds between the Hβ surface brightness and the [S II] density. Our proposed power-law stratification is therefore capable of providing a credible explanation for the intriguing [S II] density-radius correlation discovered by WO95.

4.2. *Comparison with our Long-Slit Data*

Comparison of the models with our long-slit data is made considering both the [S II] density and the Hβ surface brightness. One difficulty resides in relating the local IF radius, R_s, with position, D, along our slit. We have proceeded as follows. We have not resolved the inverse problem of finding the distance of the IF at each observed position along D.

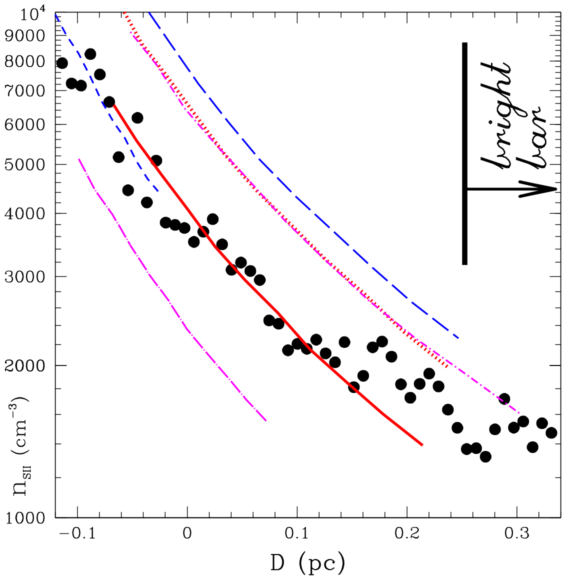

Fig. 5. Behavior of the [S II] density after projection onto our long-slit (D-axis). The slit was aligned EW. $D = 0$ corresponds to the pixel nearest to θ^1 C Ori with D increasing towards the East, crossing the Bright Bar near $D = 0.25$. The long- and short-dashed line models represent the *dust-free* case with $n_0 = 150$ and $2000\,\mathrm{cm}^{-3}$, respectively. The dotted and the solid lines represent models with internal dust using the *orion* and *noiro* curves, respectively (both with $n_0 = 150\,\mathrm{cm}^{-3}$). The two dot-dashed lines represent the *noiro* dusty model using an boundary density of $n_0 = 50\,\mathrm{cm}^{-3}$ (short-dash dotted line) and $500\,\mathrm{cm}^{-3}$ (long-dash dotted line), respectively.

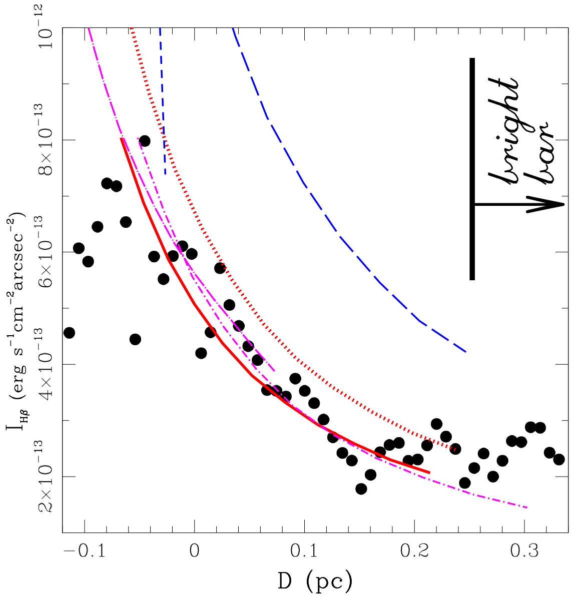

Fig. 6. Behavior of the Hβ surface brightness in power-law density stratified models after projection onto our long-slit. The long-dash and short-dash lines represent *dust-free* models with $n_0 = 150$ and $2000\,\mathrm{cm}^{-3}$, respectively. The dotted and solid line (both with $n_0 = 150\,\mathrm{cm}^{-3}$) are models with internal dust using the *orion* and *noiro* curves, respectively. The two dot-dash lines represent the *noiro* dusty model with boundary densities of $n_0 = 50\,\mathrm{cm}^{-3}$ (short-dash dotted line) and $500\,\mathrm{cm}^{-3}$ (long-dash dotted line), respectively. The observed Hβ surface brightnesses plotted here have been reduced to correct for the contribution of the scattered light (§ 3.3) and for the contribution of the foreground component (§ 3.2), as in WO95 and BF91, respectively.

Our main goal consists rather in exploring whether a power-law density is generally consistent with the data at hand. With this perspective in mind, we settled for the following simple relation between D and R_s : $D = \sqrt{R_s^2 - 0.073^2\,\mathrm{pc}} - d$, where $0.073\,\mathrm{pc}$ is the slit offset of $30''$ to the South, R_s is the true IF distance to θ^1 C Ori for a given slit position, D, in parsec projected on the sky. $D = 0$ corresponds to the pixel nearest to θ^1 C Ori, with D increasing towards the East. The additional parameter d (in pc) was obtained by iteration, using as a constraint that our best model should fit as closely as possible both the observed [S II] densities and the Hβ surface brightnesses. If the IF lay on a perfect plane perpendicular to our line-of-sight, then d would correspond to the substellar distance (O'Dell 1994), and it would have to be subtracted in quadrature from r (as for the slit offset). This resulted, however, in an unsatisfactory fit for all the models tried. A plausible explanation can be found in the 3D map of the IF shape of WO95 which shows that the IF plane is tilted away from us at the corresponding position of our slit. The above equation, in which d is subtracted linearly, qualitatively describes a tilted plane. A cartoon describing the proposed IF geometry is shown in Figure 4.

In Figure 5, we compare our stratified models with the [S II] densities observed along the slit. For simplicity, all models cover the same range in L, from 0.22 to 0.66 pc, which is the appropriate range for the favored solid line model. This has the advantage of clarifying the effect of varying only one parameter at a time (either n_0 or μ_D). The surface brightnesses along the slit are shown in Figure 6 and can be compared with the various model sequences. The two figures were drawn using $d = 0.26$, which is the value required by the favored model (solid line).

We emphasize that no dust-free model could provide an acceptable fit to the data in both Figs. 5 and 6, whatever value was used for d. In the case of dusty models using the alternative extinction curve *orion*, the fit was never satisfactory for both figures simultaneously. In effect, if we increase d to 0.35, this shifts all model sequences to the left by 0.09 pc in both figures, thereby resulting in a good fit for the *orion* model in Fig. 5 but at the expense of an unsatisfactory fit in Fig. 6. Increasing the dust content brings the dusty models down, but this is not possible in the case of the *orion* since $\mu_{\rm D} = 0.8$ is already the maximum allowed given the subsolar metallicity of Orion. The preeminence of small grains, on the other hand, has the advantage that less dust is necessary ($\mu_{\rm D} = 0.4$ for the *noiro* curve). This scenario makes sense in the event that dust grains have been progressively photoeroded.

In conclusion, even when allowing d to vary freely, the Orion model consisting of boundary density $n_0 = 150\,{\rm cm}^{-3}$ and containing small grains (*noiro* with $\mu_{\rm D} = 0.4$) provides the optimal set of physical conditions[5] favored by our model for the following reasons:

1. Dust-free models are unsuccessful in reproducing the observed behavior of the Hβ surface brightness of Fig. 6 (adopting a larger value for $Q_{\rm H}$ would worsen the discrepancy).
2. For a given dust content and size distribution, the determination of the boundary density n_0 is straightforward since the curves using different densities lie relatively far apart in the [S II] density diagram of Fig. 5 (for instance, compare the position of the two dash-dotted lines corresponding to sequences with boundary densities of $n_0 = 50$ or $500\,{\rm cm}^{-3}$),
3. Models favoring the preeminence of small grains (e.g. the *noiro* extinction) provide a simultaneous fit to both data sets presented in Figs. 5 and 6, respectively.

The applicability of the proposed model does not include the so-called "Bright Bar" (≥ 0.25 pc) beyond which the Hβ brightness is slightly rising. Accounting for this rise in our simple picture would require a gas structure which lies closer to θ^1 C Ori than the calculated IF model above. Alternatively, the rise may be due to some sort of limb brightening. For example, Dopita, Dyson, & Meaburn (1974) have proposed that the Bright Bar corresponds to the IF seen edge-on. This is qualitatively corroborated by the IF distance map produced by WO95, which shows a sharp ridge at the position of the Bar.

[5]Interestingly, the apparent reddening manifested in the emergent line ratios due to internal dust is very small. In effect, the emergent Balmer decrement for the small-grain and the dust-free models are 2.97 and 2.88 respectively

4.3. *Gas Temperature and Line Ratios*

Although the present work does not attempt to provide a fit to all of the observed line ratios, it is worth checking whether the proposed power-law density stratification results in ratios similar to those observed. Because the ionization parameter in our models is not a free parameter, line ratios become an interesting consistency check. Furthermore, it is worth testing whether the models can reproduce the observed line ratio trends with slit position.

In a similar fashion to BF91, one important parameter of our models is the stellar temperature which directly affects the excitation line ratio [O III]/Hβ. We found that satisfactorily reproducing this ratio requires a stellar temperature of 38000 K when using the stellar atmosphere models[6] of Hummer & Mihalas (1970). This temperature is consistent with an evolved star of spectral type O7 (cf. WO95). Our line ratio calculation of [O III]/Hβ is represented by the solid line in Figure 7*d* using the same parameters as before, that is, a boundary density $n_0 = 150\,{\rm cm}^{-3}$ and an extinction curve consisting of small grains (*noiro*), with $\mu_{\rm D} = 0.4$. We discuss below possible explanations for the solid line lying slightly below the data. In any event, it is encouraging that the models show the same gradient as the data.

As for the temperature indicators $R_{\rm N\,II}$ = [N II] λ 5755 / [N II] λ 6583 and $R_{\rm O\,III}$ = [O III] λ 4363 / [O III] λ 5007, a gradient is also present in the data as shown by Fig. 7*bc* (BF91 reported also a gradient of $R_{\rm N\,II}$, although for a different slit alignment). According to the models, the gradient in the $R_{\rm O\,III}$ ratio is due to a temperature gradient ($\Delta T \simeq 500$ K) while in the case of Nitrogen it is due to both a density gradient (via collisional deexcitation, cf. BF91) and a temperature gradient. Although the stratified models can successfully fit the observed trends in Fig. 7*bc*, the predicted ratios lie somewhat lower than observed, more so for $R_{\rm O\,III}$. Lowering the metallicity would increase $R_{\rm O\,III}$ but at the expense of having the [O III]/Hβ ratio becoming larger than observed.

[6]More recent stellar atmosphere models exist (Hubeny & Lanz 1995; Schaerer & de Koter 1997; Hillier & Miller 1998; Pauldrach et al. 2001) but they differ considerably according to whether they include the effect of stellar winds or not, cf. Fig. 5 in Sankrit & Hester (2000). Until the issue of wind loss is resolved, all stellar temperatures inferred from photoionization models will be of limited accuracy. The models of Hummer & Mihalas were used above for their convenience as they can be interpolated to any arbitrary temperature within MAPPINGS IC. Our results do not depend on which family of models is used provided the stellar temperature is adjusted to reproduce the line ratios well.

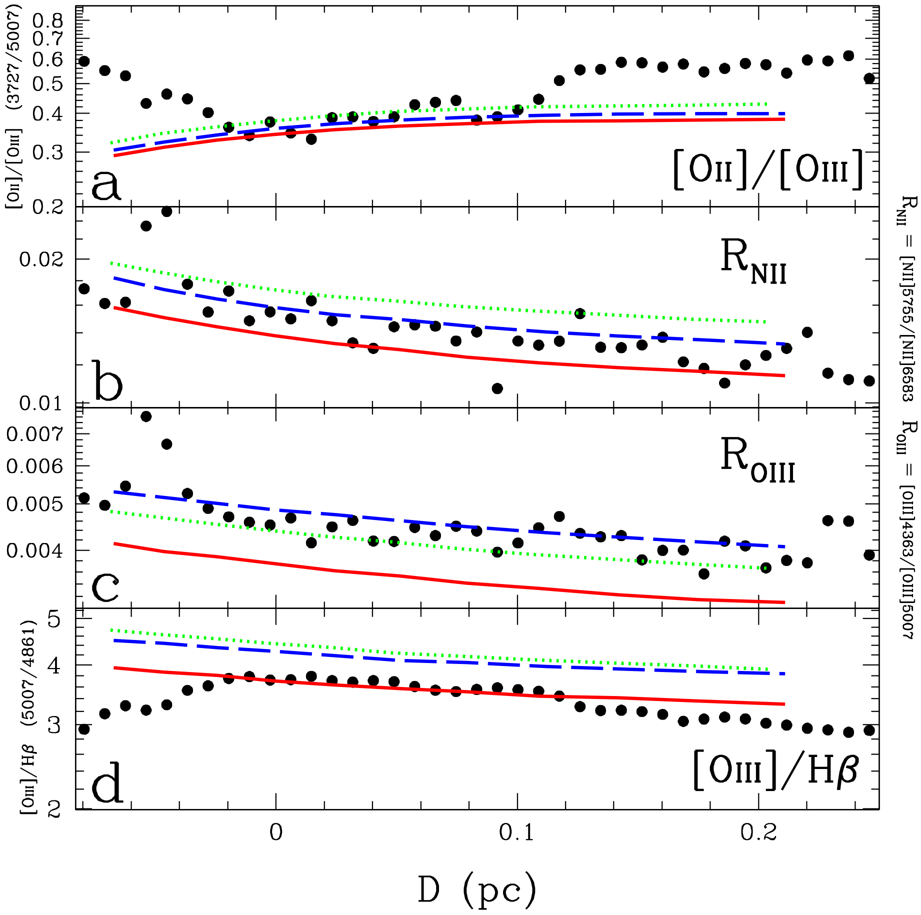

Fig. 7. Observed line ratio (dots) compared with model predictions. (a) The line ratio [O II] $\lambda\lambda$ 3727/[O III] λ 5007, which is a good indicator of the degree of ionization. (b) The Nitrogen temperature-sensitive ratio [N II] λ 5755/[N II] λ 6583. (c) The Oxygen temperature-sensitive ratio [O III] λ 4363/[O III] λ 5007. (d) The [O III] λ 5007/Hβ λ4861 ratio. The vertical scales in (b), (c,) and (d) are the same and extend over 0.42 dex. The model predictions are indicated by lines (see § 4.3): the solid line shows the behavior of line ratios along the slit for our most successful model ($n_0 = 150$ cm^{-3} and the *noiro* curve with $\mu_D = 0.4$). The long-dashed line was calculated assuming temperature fluctuations with $t^2 = 0.01$. The dotted line was calculated using half the diffuse field from the "outward-only" approximation. The spike in the data near $D = -0.05$ pc in (b) and (c) is believed to be due to a foreground proplyd.

It is well known that photoionization models do not explain why the temperatures derived from collisionally excited lines differ from those derived from recombination lines (see review by Peimbert 1995). In the case of Orion, Esteban et al. (1998) found that the abundance of the O^{+2} ion derived from the O II recombination lines is incompatible with the same ion abundance derived from collisionally excited [O III] λ 5007 when a common temperature is adopted. Deriving a unique ionic abundance was found to require different *mean* temperatures. These can be justified if there exist high amplitude temperature fluctuations in the nebula (Peimbert 1967), which far exceed the amplitude arising from traditional photoionization models (Kingdon & Ferland 1995, 1998; Pérez 1997). The mean square fluctuation amplitudes that Esteban et al. (1998) inferred lie in the range $t^2 = 0.02$–0.028. The effect of temperature fluctuations on line emissivities was incorporated into the MAPPINGS Ic code by the scheme described in Binette & Luridiana (2000). The long-dashed lines in Fig. 7 represent such a model calculated with $t^2 = 0.01$. As expected, $R_{\rm N\,II}$ and, more so, $R_{\rm O\,III}$ are both significantly increased and can now reproduce satisfactorily the data of Fig. 7*bc*. The calculated [O III]/Hβ ratio in Fig. 7*a*, however, now lies too high, and the stellar temperature would have to be reduced in order to produce a selfconsistent model in all panels of Fig. 7. Given our current poor knowledge about the nature and cause of the postulated temperature fluctuations, we have not carried out the iterative process any further.

The diffuse ionization radiation field has a non-negligible impact on the gas temperature. In our models, we use the "outward-only" approximation to treat the transfer of the diffuse radiation. This is equivalent to assuming a single direction for the propagation of the diffuse field, a technique based on the approximation that the diffuse field is soft and does not therefore travel far from the point of emission. To test whether the integration along the direction of increasing density may cause an overestimation of the intensity of the diffuse radiation, we have calculated models in which we reduced by half the strength of the diffuse field (adopting $t^2 = 0$). Such models are represented by the dotted lines in Fig. 7. We can see a significant shift, which is in the same direction as that caused by temperature fluctuations with $t^2 \sim 0.01$. The dotted lines give us useful upper limits on the line ratio uncertainties resulting from a possible inadequacy of the outward-only approximation.

Fig. 7*a* is a plot of the [O II]/[O III] ratio. The models can reproduce the observed points only within a restricted slit range. No obvious explanation can be found for the discrepancy outside it. It possibly reflects the limitations of our simplified geometry, as discussed in § 3.2, or the larger errors affecting the UV [O II] lines. Overall, the fit of the gradients using our simple models appears satisfactory in all the panels of Fig. 7.

5. CONCLUSIONS

The method used by WO95 to determine the IF shape requires, at each point of the nebula, knowledge of *both* the Hα surface brightness and the IF density (using the [S II] or [O II] doublet). For a power-law density stratification as proposed in this paper, the density across the nebula is not a free parameter since it is uniquely determined by the local power-law scale L. This opens up the possibility that using only the Hα (or Hβ) surface brightness map, one could, in principle, determine the IF shape of the whole nebula. For this reason, further studies are warranted in order to: (a) extend the comparison of power-law density models to a more extensive set of observations of Orion and (b) work out a scheme to solve for the inverse problem (as was done by WO95 in the exponential case) in order to determine the IF shape assuming the proposed power-law density gradient and taking into account the effects of internal dust.

LB and YDM acknowledge financial support from the CONACyT grants 32139-E and 25869-E, respectively. We are thankful to M. Rodríguez for sharing detailed information about her spectroscopic observations of Orion. We also thank the unknown referee for the many constructive comments made to the original draft.

REFERENCES

Baldwin, J. A., et al. 1991, ApJ, 374, 580 (BF91)
Bertoldi, F. 1989, ApJ, 346, 735
Bertoldi, F., & Draine, B. T. 1996, ApJ, 458, 222
Binette, L., & Luridiana, V. 2000, RevMexAA, 36, 43
Binette, L., & Raga, A. 1990, AJ, 100, 1046 (BR90)
Binette, L., Wang, J., Villar-Martin, M., & Magis C. G. 1993, ApJ, 414, 535
Dopita, M. A., Dyson, J., & Meaburn, J. 1974, Ap&SS, 28, 61
Esteban, C., Peimbert, Torres-Peimbert, S., & Escalante, V. 1998, MNRAS, 295, 401
Franco, J., García-Barreto , A., & de la Fuente, E. 2000a, ApJ, 544, 277
Franco, J., Kurtz, S., Hofner, P., Testi, L., García-Segura, G., & Martos, M. 2000b, ApJ, 542, 143
Franco, J., Tenorio-Tagle, G., & Bodenheimer, P. 1989, RevMexAA, 18, 65
_________. 1990, ApJ, 349, 126
González-Gómez, D. I. 1999, Undergraduate thesis, Universidad Autónoma de Puebla, México
Hester, J. J., et al. 1996, AJ, 111, 2349
Hillier, D. J., & Miller, D. L. 1998, ApJ, 496, 407
Hubeny, I., & Lanz, T. 1995, ApJ, 439, 875
Hummer, D. G., & Mihalas, D. M. 1970, MNRAS, 147, 339
Kingdon, J. B., & Ferland, G. J. 1995, ApJ, 450, 691
_________. 1998, ApJ, 506, 323
Magris C. G., Binette, L., & Martin, P. G. 1993, Ap&SS, 205, 141
Martin, P. G., & Rouleau, F. 1991, in First Berkeley Colloquium on Extreme Ultraviolet Astronomy, eds. R. F. Malina & S. Bowyer (New York: Pergamon Press), 341
Münch, G. 1958, Rev. Mod. Phys., 30, L1035
O'Dell, C. R. 1994, Ap&SS, 216,267
Pauldrach, A. W. A., Hoffmann, T. L., & Lennon, M. 2001, A&A, 375, 161
Peimbert, M. 1967, ApJ, 150, 825
_________. 1995, in The Analysis of Emission Lines, ed. R. E. Williams & M. Livio (Cambridge: Cambridge University Press), 165
Pérez, E. 1997, MNRAS, 290, 465

Richling, S., & Yorke, H. W. 2000, ApJ, 539, 258
Rodriguez, M. 1999, A&A, 351, 1075
Sankrit, R., & Hester, J. J. 2000, ApJ, 535, 847
Schaerer, D., & de Koter, A. 1997, A&A, 322, 598
Seaton, M. J. 1979, MNRAS, 187, 73P
Shields, G. A., & Searle, L. 1978, ApJ, 222, 821
Stasińska, G., & Szczerba, R. 2001, A&A, 379, 1024
Tenorio-Tagle, G. 1979, A&A, 7, 59
Wen, Z., & O'Dell, C. R. 1995, ApJ, 438, 784 (WO95)
Williams, R. E. 1992, ApJ, 392, 99
Wurm, K. 1961, Zeit. Ap., 52, 149
Yorke, H. W. 1986, ARA&A, 24, 49

L. Binette and D. I. González-Gómez: Instituto de Astronomía, UNAM, Apdo. Postal 70-264, 04510 México D.F., México (binette, dulce@astroscu.unam.mx).
Y. D. Mayya: Instituto Nacional de Astrofísica, Optica y Electrónica, Apdo. Postal 216, 7200 Puebla, Puebla, México.